

## Short Communication

# The First Autopsy Case of Pandemic Influenza (A/H1N1pdm) Virus Infection in Japan: Detection of a High Copy Number of the Virus in Type II Alveolar Epithelial Cells by Pathological and Virological Examination

Noriko Nakajima<sup>1</sup>, Satoru Hata<sup>2</sup>, Yuko Sato<sup>1</sup>, Minoru Tobiume<sup>1</sup>, Harutaka Katano<sup>1</sup>, Keiko Kaneko<sup>1</sup>, Noriyo Nagata<sup>1</sup>, Michiyo Kataoka<sup>1</sup>, Akira Aina<sup>3</sup>, Hideki Hasegawa<sup>1,3</sup>, Masato Tashiro<sup>3</sup>, Makoto Kuroda<sup>4</sup>, Tamami Odai<sup>5</sup>, Nobuyuki Urasawa<sup>5</sup>, Tomoyoshi Ogino<sup>6</sup>, Hiroaki Hanaoka<sup>6</sup>, Masahide Watanabe<sup>6</sup>, and Tetsutaro Sata<sup>1\*</sup>

<sup>1</sup>Department of Pathology, <sup>3</sup>Influenza Virus Research Center, and <sup>4</sup>Pathogen Genomics Center, National Institute of Infectious Diseases, Tokyo 162-8640; and <sup>2</sup>Department of Clinical Laboratory, <sup>5</sup>Department of Cardiology, and <sup>6</sup>Department of Pathology, Nagano Red Cross Hospital, Nagano 380-8582, Japan

(Received December 15, 2009. Accepted January 5, 2010)

**SUMMARY:** We report the pathological and virological findings of the first autopsy case of the 2009 pandemic influenza (A/H1N1pdm) virus infection in Japan. A man aged 33 years with chronic heart failure due to dilated cardiomyopathy, mild diabetes mellitus, atopic dermatitis, bronchial asthma, and obesity died of respiratory failure and multiple organ dysfunction syndrome. Macroscopic examination showed severe pulmonary edema and microscopically the lung sections showed very early exudative-stage diffuse alveolar damage (DAD). Immunohistochemistry revealed proliferation of the influenza (A/H1N1pdm) virus in alveolar epithelial cells, some of which expressed SA $\alpha$ 2-3Gal on the cell surface. Influenza (A/H1N1pdm) virus genomic RNA and mRNA were also detected in alveolar epithelial cells. Real-time PCR revealed 723 copies/cell in the left lower lung section from which the influenza (A/H1N1pdm) virus was isolated. Electron microscopic analysis revealed filamentous viral particles in the lung tissue. The concentrations of various cytokines/chemokines in the serum and the autopsied lung tissue were measured. IL-2R, IL-6, IL-8, IL-10, IFN- $\alpha$ , MCP-1, and MIG levels were elevated in both. These findings indicated a case of viral pneumonia caused by influenza (A/H1N1pdm) virus infection, showing characteristic pathological findings of the early stage of DAD.

The 2009 pandemic influenza (A/H1N1pdm) virus causes severe respiratory disease, neurologic complications, and myocardial symptom in some patients (1–3). From August 15 through December 15, 2009, a total of 116 patients with confirmed infection with influenza (A/H1N1pdm) virus died in Japan (4). Autopsy verification of the cause of death is indispensable to elucidate the pathogenesis of influenza (A/H1N1pdm) virus infection. Pathological findings of fatal influenza (A/H1N1pdm) virus infection have recently been reported (5,6). Here, we report in detail the pathological and virological findings of the first autopsy case in Japan.

On August 20, 2009 (day 1), a man aged 33 years with chronic heart failure due to dilated cardiomyopathy, mild diabetes mellitus, atopic dermatitis, asthma, and obesity (BMI, 38) complained of cough and watery diarrhea. On day 6, he was admitted with progressive dyspnea, high fever (39°C) and diarrhea. On admission, a chest radiograph showed nodular infiltrates in the lower lungs (Fig. 1a) and a chest computed tomography (CT) scan revealed severe bilateral consolidations (Fig. 1b). The leukocyte count was 5,210/mm<sup>3</sup> and CRP was 1.1 mg/dl. The nasopharyngeal swab specimens were negative for influenza virus type A antigen by the rapid test (ESPLINE<sup>®</sup> Influenza A&B Kit; Fujirebio, Tokyo,

Japan), and therefore oseltamivir was not administered. On the morning of day 7, the patient required intubation and was placed on mechanical ventilation. At intubation, foamy, white and partly bloody fluid spouted out from the tube. Methylprednisolone pulse therapy and administration of a neutrophil elastase inhibitor (sivelestat sodium hydrate) were initiated for the treatment of acute respiratory distress syndrome (ARDS). The diagnosis of influenza (A/H1N1pdm) virus infection was confirmed by real-time reverse transcriptase-polymerase chain reaction (RT-PCR) testing on day 7. In spite of intensive care, the patient died of respiratory failure and multiple organ dysfunction syndrome on day 8. The chest radiograph showed progressive and confluent consolidations (Fig. 1c).

Autopsy revealed macroscopically severe pulmonary edema, hemorrhage, exudation and focal nodular lesions in the lungs (left, 730 g; right, 800 g) (Fig. 2a). The bilateral main bronchi were filled with foamy liquid, which was positive for influenza virus A antigen. The nodular lesions were palpable in the lower lungs, and corresponded to the nodular shadows of the chest radiographic findings (Fig. 1c). The heart was enlarged and all chambers were dilated (670 g), and the left ventricular wall and septal wall had irregular whitish patches, compatible with dilated cardiomyopathy (Figs. 2b and c). The brain was edematous and swollen (1,350 g). Hyperplastic solitary lymph follicles of the terminal ileum and rectal erosion were observed.

Tissue samples from all major organs were fixed in 20% buffered formalin and embedded in paraffin by an automated

\*Corresponding author: Mailing address: Department of Pathology, National Institute of Infectious Diseases, 1-23-1 Toyama, Shinjuku-ku, Tokyo 162-8640, Japan. Tel: +81-3-5285-1111, Fax: +81-3-5285-1189, E-mail: tsata@nih.go.jp

processor (SAKURA ETV-150CV; Sakura Finetek Japan, Tokyo, Japan). Each section was cut into 3  $\mu\text{m}$  in thickness, mounted on silane-coated slides (Matsunami, Tokyo, Japan) and was examined histologically. Hematoxylin and eosin-

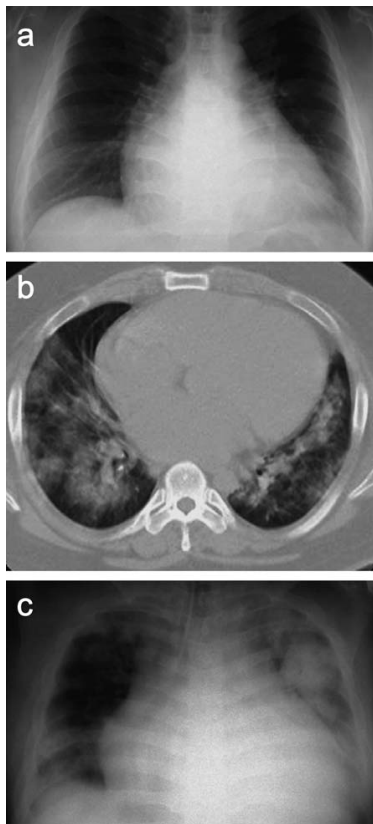


Fig. 1. Radiograph of the lung and chest computed tomography (CT). (a) The radiograph showed nodular infiltrates in lower lungs on day 6. (b) The chest CT scan revealed severe bilateral consolidations on day 6. (c) The radiograph showed progressive and confluent consolidations on day 8.

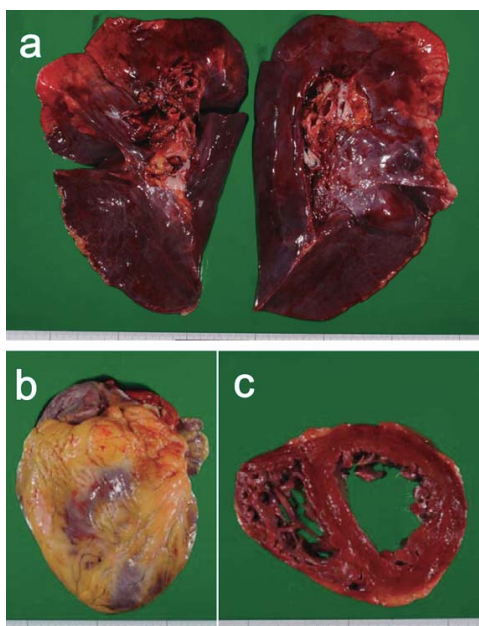


Fig. 2. Macroscopical findings. (a) Pulmonary edema (left, 730 g; right, 800 g). (b, c) Enlarged heart (670 g) and dilated chambers compatible with dilated cardiomyopathy.

stained lung sections demonstrated intra-alveolar edema with fibrin, erythrocytes and desquamated epithelial cells in alveolar spaces, hyperplasia of type II pneumocytes, and hemosiderin-laden macrophages (heart failure cells) (Figs. 3a, b, c, d, and e). No viral inclusion bodies or cytopathic changes were observed in pneumocytes. Neutrophil infiltration was not prominent. Regenerative hyperplasia and desquamation of the pseudostratified columnar epithelium of the bronchi were observed (Fig. 3a). Some sections demonstrated the feature of early exudative-stage diffuse alveolar damage (DAD) with hyaline membrane formation (Fig. 3c). The findings of more progressed proliferative-stage DAD were also observed in a few sections (Fig. 3e).

To evaluate the distribution of influenza (A/H1N1pdm) virus antigen, all sections were immunostained by an avidin-biotin complex immunoperoxidase method (LSAB2 kit/HRP/DAB; Dako Cytomation, Copenhagen, Denmark) using a mouse monoclonal antibody against influenza A nucleoprotein (InfA-NP) (7). Positive signals for InfA-NP antigen were detected primarily in the lung field sections, and only sparsely in a bronchial section (Figs. 3f, g, h, and i). No signals were detected in a trachea section or the other extrapulmonary tissue sections. Many viral antigen-positive cells were detected in the earlier-stage DAD lesions before hyaline membrane formation (Figs. 3f, g, h, and i) rather than in the progressed lesions (Fig. 3j). The signals were found in alveolar epithelial cells, both type I and type II pneumocytes (Figs. 3b, d, g, and i). The influenza (A/H1N1dm) virus genomic RNA (minus-strand RNA) and mRNA (plus-strand RNA) were detected in the same lesion by the in situ hybridization AT-tailing CSA (ISH-AT-CSA) method using strand-specific oligonucleotide probes for the NP region of the influenza (A/H1N1pdm) virus (sense probe: 5'-gcaaggttcaacacttcccagaaggctggtgccgaggt-ATATATATATATATATAT-3', anti-sense probe: 5'-acctcggcaccagaccttctgggaagtgtgaaaccttgc-ATATATATATATATATAT-3') (Figs. 4a and b) (8,9). This revealed that the virus had replicated in the alveolar epithelial cells. No signals were detected using an irrelevant probe as a negative control (Fig. 4c).

To characterize the virus-infected cells, confocal laser scanning microscopy was used to visualize double immunofluorescence staining for InfA-NP and for the cell type-specific marker proteins EMA (epithelial cells), SP-D (type II pneumocytes), cytokeratin AE1/AE3 (epithelial cells), CD68 (macrophages) and CD34 (endothelial cells) as previously described (10). Alexa Fluor 568-conjugated anti-mouse or anti-rabbit IgG (Molecular Probes, Eugene, Oreg., USA) and Alexa Fluor 488-conjugated anti-rabbit or anti-mouse IgG (Molecular Probes) were used as secondary antibodies. Almost all InfA-NP signals were detected in epithelial (EMA-positive) cells (Fig. 4d). They were also detected in SP-D-positive cells, suggesting type II pneumocytes (Fig. 4e). A few were detected in AE1/AE3-positive bronchial epithelial cells. None were detected in CD68-positive macrophages or CD34-positive endothelial cells (data not shown).

The influenza A virus binds to receptors containing terminal sialic acids linked to galactose on cell surface glycoproteins by a 2-3 linkage (SA $\alpha$ 2-3Gal) and/or by a 2-6 linkage (SA $\alpha$ 2-6Gal) (11). Swine influenza HA binds to both SA $\alpha$ 2-6Gal and SA $\alpha$ 2-3Gal (12). In the human respiratory organs, putative SA $\alpha$ 2-6Gal receptors were mainly expressed in the epithelium of the upper respiratory tract and SA $\alpha$ 2-3Gal receptors were expressed in the epithelium of the lower respiratory tract (data not shown). The sections were incubated



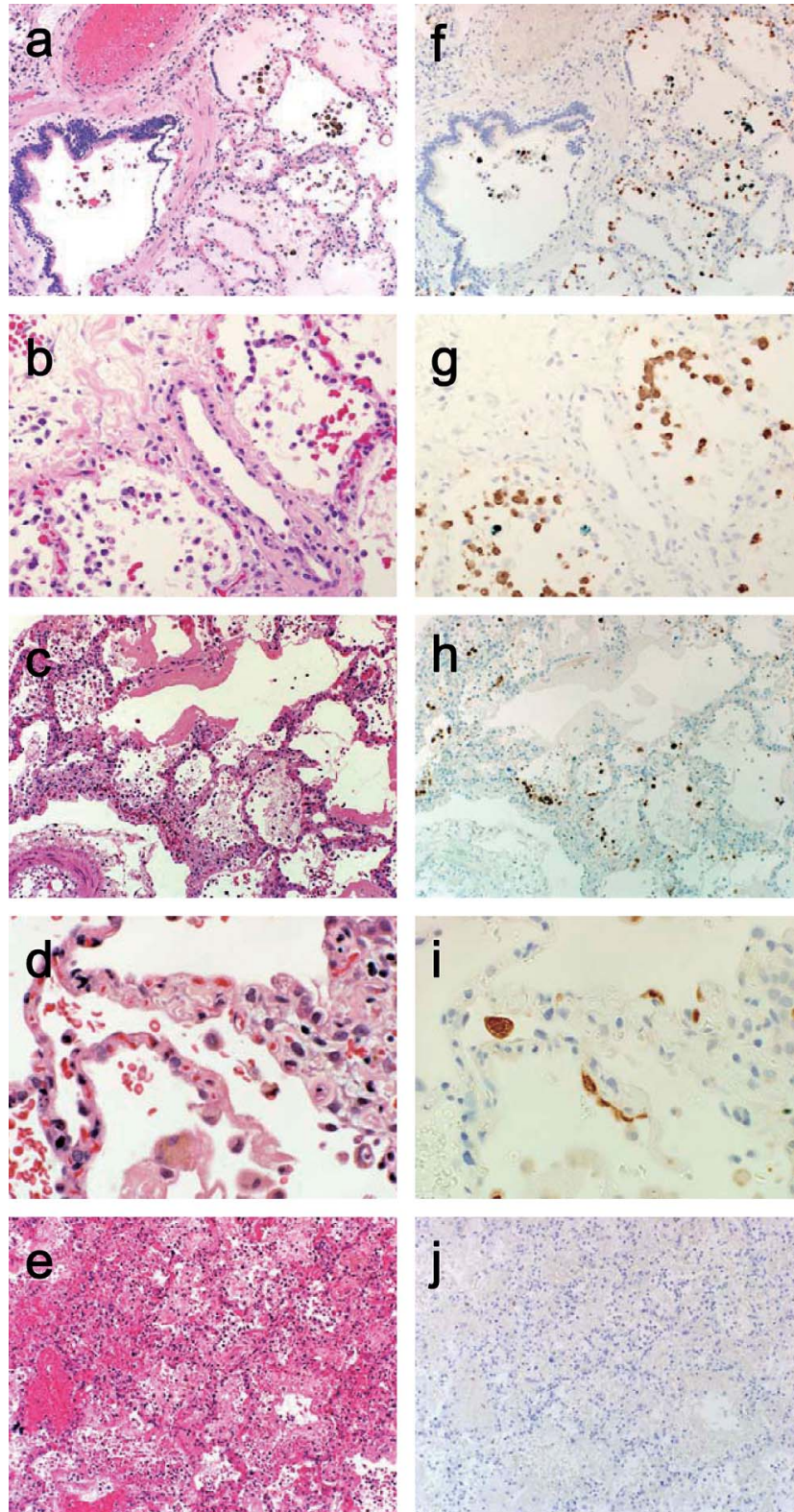


Fig. 3. Hematoxylin and eosin staining (a, b, c, d, and e) and immunohistochemistry for influenza A nucleoprotein (InfA-NP) (f, g, h, i, and j). Intra-alveolar edema with liquid, fibrin, erythrocytes and desquamated epithelial cells in alveolar spaces, hyperplasia of type II pneumocytes, and hemosiderin-laden macrophages (heart failure cells) were generally observed. (a) Regenerative hyperplasia and desquamation of the pseudostratified columnar epithelium of the bronchi were observed. (b, c, d) Early exudative-stage diffuse alveolar damage (DAD) with hyaline membrane formation. (e) More progressed proliferative-stage DAD were shown. (f, g, h, and i) A lot of viral antigen-positive cells were detected in the earlier-exudative stage DAD lesions before hyaline membranes formation. (i) The signals were also found in alveolar type I pneumocytes. (j) Few viral antigen-positive cells were detected in the progressed lesion. Original magnification,  $\times 100$  (a, c, e, f, h, and j),  $\times 200$  (b, g),  $\times 400$  (d, i).

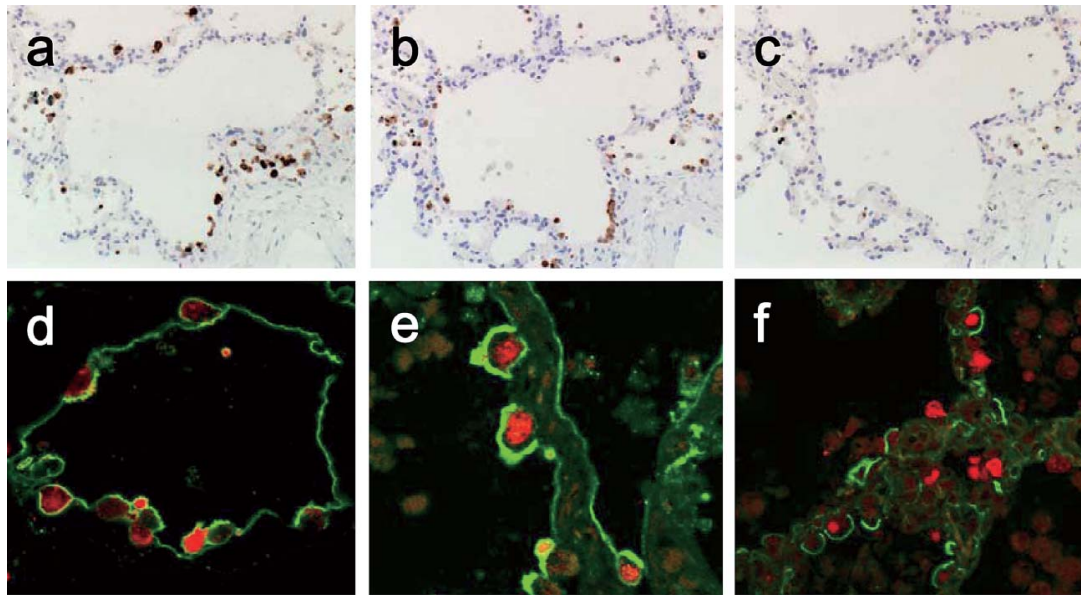


Fig. 4. The detections of influenza (A/H1N1pdm) virus-RNA using in situ hybridization AT-tailing-CSA method. (a) The influenza (A/H1N1pdm) virus genomic-RNA detected using a sense-probe. (b) The influenza (A/H1N1pdm) virus-mRNA detected using an anti-sense probe. (c) No signals were detected using an irrelevant probe. Original magnification,  $\times 200$ . Double immunofluorescence staining. (d) Influenza virus A nucleoprotein (InfA-NP) (red) and EMA for epithelial cells (green) were co-localized. (e) InfA-NP (red) and SP-D for type II pneumocytes (green) were co-localized. (f) InfA-NP (red) were detected in the cells expressing sialic acids linked to galactose by a 2-3 linkage (SA $\alpha$ 2-3Gal) (green). Original magnification,  $\times 400$ .

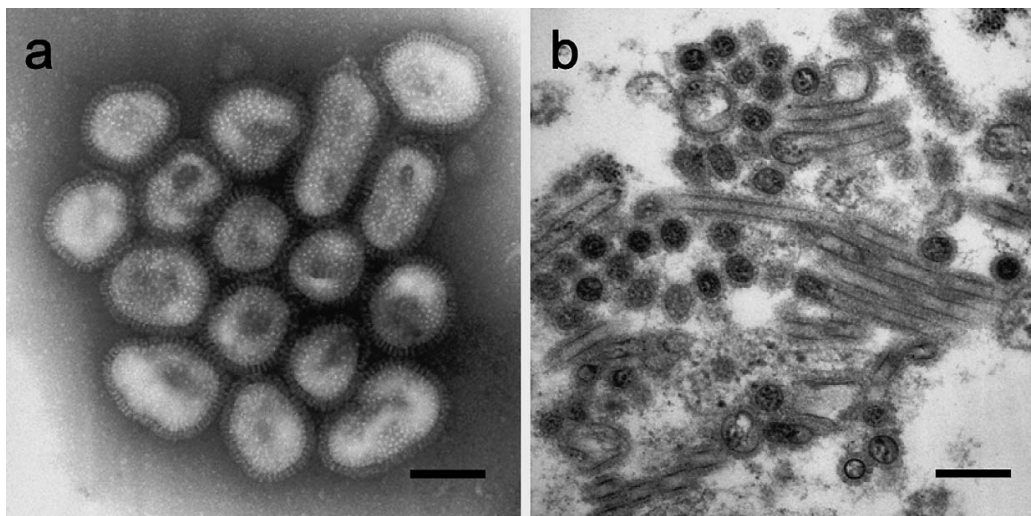


Fig. 5. Electron microscopy. (a) The negative staining feature of isolated influenza (A/H1N1pdm) virus particles in the culture supernatant. Scale bar, 100 nm. (b) The influenza (A/H1N1pdm) viral particles in filamentous forms in the lung sections. Scale bar, 200 nm.

with biotinylated-*Maackia amurensis* lectin II (MAA-II) (Vector Laboratories, Burlingame, Calif., USA) to detect SA $\alpha$ 2-3Gal and with biotinylated-*Sambucus nigra* lectin I (SNA-I) (EY Laboratories, San Mateo, Calif., USA) to detect SA $\alpha$ 2-6Gal. They were then incubated with Fluor 488-conjugated streptavidin (Molecular Probes). Double fluorescence staining and visualization with a confocal laser scanning microscope revealed that some infA-NP-positive cells expressed SA $\alpha$ 2-3Gal on the cell surface (Fig. 4f), suggesting that A/H1N1pdm HA is able to bind to SA $\alpha$ 2-3Gal receptors and to infect type II pneumocytes. Because few infA-NP are detected in bronchial epithelial cells on day 8 in this case, it was difficult to confirm that A/H1N1pdm HA was able to bind to SA $\alpha$ 2-6Gal receptors, which are abundant on the surface of bronchial epithelial cells.

To examine the copy numbers of the influenza (A/H1N1pdm) virus, RNAs extracted from 4 paraffin-embedded sections ( $5 \mu\text{m} \times 3$ ) (left upper lung, left lower lung, left bronchus, middle trachea) were identified by quantitative real-time RT-PCR using an Mx3005P system (Stratagene, La Jolla, Calif., USA), which amplified a segment within the HA region of the A/H1N1pdm virus-RNA (13). The amount of human beta-actin mRNA in the DNase-treated RNA extracted from each section was also determined as an internal reference gene to provide a normalization factor for the amount of RNA isolated from a specimen (14). To amplify A/H1N1pdm-HA, forward (swH1N1-HA-F: 5'-CCCCATTGCA TTTGGGTAAA-3') and reverse (swH1N1-HA-R: 5'-TGGA GAGTGATTCACACTGGAT-3') primers were used with a labeled probe 5'-(FAM)AACATTGCTGGCTGGATCCTG



GGA(TAMRA)-3'. Real-time RT-PCR revealed  $2.37 \times 10^5$  copies of A/H1N1pdm-RNA and  $4.92 \times 10^5$  copies of beta-actin mRNA in the left lower lung section. The beta-actin mRNA copy number was 1,500 copies/cell (unpublished data). Therefore the influenza (A/H1N1pdm) virus-RNA copy number was calculated as 723 copies/cell in the left lower lung section. Similarly, it was calculated as 10 copies/cell in the left upper lung section, 2 copies/cell in the left bronchus and less than 1 copy/cell in the middle trachea. The differences in the copy numbers of influenza (A/H1N1pdm) virus-RNA among the sections were consistent with the differences in the numbers of InfA-NP-antigen-positive cells detected by immunohistochemistry.

A/H1N1pdm virus was isolated by inoculating 20% (w/v) homogenates of the autopsy lung tissue to Madin-Darby canine kidney (MDCK) cells in the presence of trypsin. The culture supernatants were harvested on the 3rd day post-inoculation as a stock virus. The virus titer, which was expressed as 50% of the tissue culture infectious dose (TCID<sub>50</sub>)/ml on MDCK cells, was  $7.5 \times 10^5$  TCID<sub>50</sub>/ml. The whole sequence of the influenza virus proliferated in the lung was determined directly using an Illumina Genome Analyzer II (Illumina, San Diego, Calif., USA) and indirectly using the isolated strain. Both sequences mostly coincided with that of A/H1N1pdm. The former sequence was named A/Nagano/RC1-L/2009(H1N1) and the latter one was named A/Nagano/RC1/2009(H1N1). The negative staining feature of isolated A/H1N1pdm virus particles in the culture supernatant by electron microscopy (EM) is shown in Fig. 5a. In the lung tissue processed routinely for EM (15), outside of type II alveolar epithelial cells, influenza virus particles in filamentous rather than spherical forms were found (Fig. 5b).

The concentration of various cytokines/chemokines in the serum on day 5 and the autopsied lung tissue were measured by using a Human Cytokine 25-plex (BioSource International, Inc., Carmarillo, Calif., USA) and Luminex100TM (Luminex Co., Austin, Texas, USA) as described previously (16). IL-2R, IL-6, IL-8, IL-10, IFN- $\alpha$ , MCP-1, and MIG levels were elevated both in the serum on day 5 before corticosteroid treatment and the autopsy lung tissue on day 8. In addition to these data, an increase of IP-10 was observed in the serum and an increase of IFN- $\gamma$  was detected in the lung tissue.

The patient had multiple risk factors for severe complications of influenza (A/H1N1pdm) virus infection, suggesting that he died of respiratory failure due to severe pulmonary edema caused by both chronic heart failure and influenza pneumonia. The lung sections showed very early exudative-stage DAD before hyaline membrane formation. Unexpectedly, a high level of proliferation of influenza (A/H1N1pdm) virus was detected in alveolar epithelial cells by immunohistochemistry, as shown in Fig. 3. We were able to detect this early stage of the disease even in the autopsied lung sections. This case provide clues to the pathogenesis of influenza pneumonia and suggests what occurs in the lungs

after influenza (A/H1N1pdm) virus infection.

#### ACKNOWLEDGMENTS

This study was supported by the Health and Labour Sciences Research Grants on Emerging and Re-emerging Infectious Diseases (to TS and NN, No. H20-Shinko-Ippan-006 and H19-Shinko-Ippan-005) from the Ministry of Health, Labour and Welfare of Japan.

We thank Drs. Takahiro Tsuji, Naoko Iwata, and Yuko Sasaki for their technical assistance, and Dr. Toshio Kumasaka for valuable discussions.

#### REFERENCES

- Centers for Disease, Control and Prevention (2009): Intensive-care patients with severe novel influenza A(H1N1) virus infection—Michigan. *Morbidity and Mortality Weekly Report*, 58, 749–752.
- Centers for Disease, Control and Prevention (2009): Neurologic complications associated with novel influenza A (H1N1) virus infection in children—Dallas, Texas. *Morbidity and Mortality Weekly Report*, 58, 773–778.
- Perez-Padilla, R., de la Rosa-Zamboni, D., Ponce de Leon, S., et al. (2009): Pneumonia and respiratory failure from swine-origin influenza A (H1N1) in Mexico. *N. Engl. J. Med.*, 361, 680–689.
- Ministry of Health, Labour and Welfare, Japan: Situation of H1N1 in Japan. Online at <<http://www.mhlw.go.jp/za/0806/c17/c17.html>>.
- Mauda, T., Hajjar, L.A., Callegari, G.D., et al. (2010): Lung pathology in fatal novel human influenza A (H1N1) infection. *Am. J. Respir. Crit. Care Med.*, 181, 72–79.
- Gill, J.R., Sheng, Z.M., Ely, S.F., et al. (2010): Pulmonary pathologic findings of fatal 2009 pandemic influenza A/H1N1 viral infections. *Arch. Pathol. Lab. Med.*, 134 (published online).
- Chen, Z., Sahashi, Y., Matsuo, K., et al. (1998): Comparison of the ability of viral protein-expressing plasmid DNAs to protect against influenza. *Vaccine*, 16, 1544–1549.
- Nakajima, N., Ionescu, P., Sato, Y., et al. (2003): In situ hybridization AT-tailing with catalyzed signal amplification for sensitive and specific in situ detection of human immunodeficiency virus-1 mRNA in formalin-fixed and paraffin-embedded tissues. *Am. J. Pathol.*, 162, 381–389.
- Nakajima, N., Asahi-Ozaki, Y., Nagata, N., et al. (2003): SARS coronavirus-infected cells in lung detected by new in situ hybridization technique. *Jpn. J. Infect. Dis.*, 56, 139–141.
- Liem, N.T., Nakajima, N., Phat, L.P., et al. (2008): H5N1-infected cells in lung with diffuse alveolar damage in exudative phase from a fatal case in Vietnam. *Jpn. J. Infect. Dis.*, 61, 157–160.
- Shinya, K., Ebina, M., Ono, M., et al. (2006): Avian flu: influenza receptors in the human airway. *Nature*, 440, 435–436.
- Gambaryan, A.S., Tuzikov, A.B., Piskarev, V.E., et al. (1997): Specification of receptor-binding phenotypes of influenza virus isolates from different hosts using synthetic sialylglycopolymers: non-egg-adapted human H1 and H3 influenza A and influenza B viruses share a common high binding affinity for 6'-sialyl (N-acetyl)lactosamine. *Virology*, 232, 345–350.
- Katano, H., Ito, H., Suzuki, Y., et al. (2009): Detection of Merkel cell polyomavirus in Merkel cell carcinoma and Kaposi's sarcoma. *J. Med. Virol.*, 81, 1951–1958.
- Kuramochi, H., Hayashi, K., Uchida, K., et al. (2006): Vascular endothelial growth factor messenger RNA expression level is preserved in liver metastases compared with corresponding primary colorectal cancer. *Clin. Cancer Res.*, 12, 29–33.
- Tobiume, M., Sato, Y., Katano, H., et al. (2009): Rabies virus dissemination in neural tissues of autopsy cases due to rabies imported into Japan from Philippines: immunohistochemistry. *Pathol. Int.*, 59, 555–566.
- Nagata, N., Iwata, N., Hasegawa, H., et al. (2008): Mouse-passaged severe acute respiratory syndrome-associated coronavirus leads to lethal pulmonary edema and diffuse alveolar damage in adult but not young mice. *Am. J. Pathol.*, 172, 1625–1637.